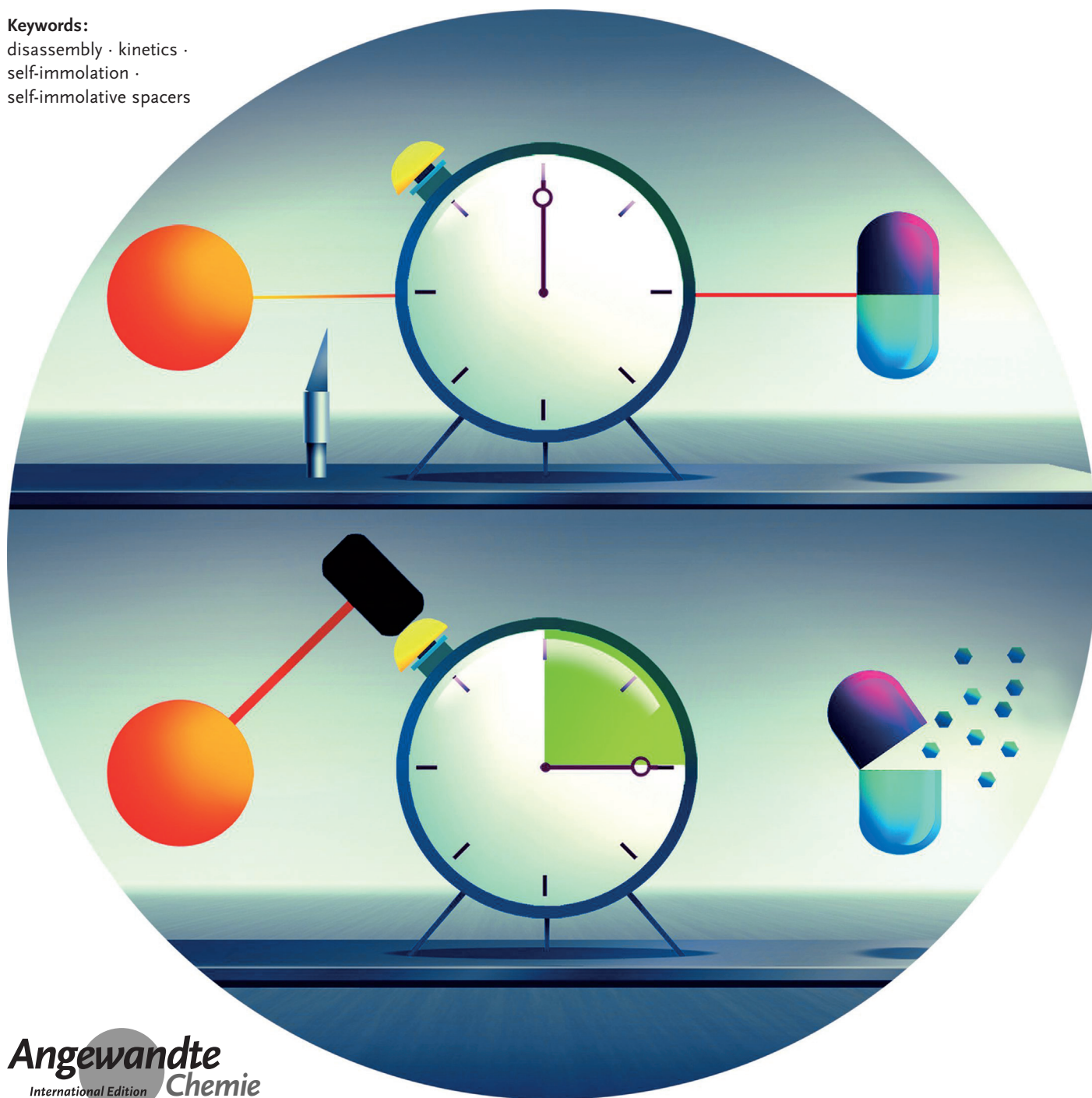


Self-Immolative Spacers: Kinetic Aspects, Structure–Property Relationships, and Applications

Ahmed Alouane, Raphaël Labruère, Thomas Le Saux, Frédéric Schmidt,* and Ludovic Jullien*

Keywords:

disassembly · kinetics ·
self-immolation ·
self-immolative spacers



Self-immolative spacers are covalent assemblies tailored to correlate the cleavage of two chemical bonds after activation of a protective part in a precursor: Upon stimulation, the protective moiety is removed, which generates a cascade of disassembling reactions leading to the temporally sequential release of smaller molecules. Originally introduced to overcome limitations for drug delivery, self-immolative spacers have gained wide interest in medicinal chemistry, analytical chemistry, and material science. For most applications, the kinetics of the disassembly of the activated self-immolative spacer governs functional properties. This Review addresses kinetic aspects of self-immolation. It provides information for selecting a particular self-immolative motif for a specific demand. Moreover, it should help researchers design kinetic experiments and fully exploit the rich perspectives of self-immolative spacers.

1. Introduction

Spatio-temporal control over the release of chemicals is a major interest in chemistry. For example, in biomedical applications, it may be useful to mask the biological activity of an active compound before it reaches its target. This strategy permits to overcome limitations of free small molecules such as low water solubility, lack of specificity to the target, or sub-optimal pharmacokinetics. Protecting groups, well-established in organic chemistry, can be useful to engineer such prodrugs: protection induces a decrease or elimination of the biological activity, the masked compound is then released under specific biological conditions.^[1–8] Hence various strategies have been used to directly release active compounds from their protected precursors. However, when the protecting group or the active compound is bulky, precursor activation may become difficult and the release of the desired compound not effective.^[9] To overcome this limitation, an efficient and increasingly popular approach consists of decoupling precursor activation from compound release by introducing a “self-immolative spacer” between the protecting group and the active compound.^[10]

Self-immolative spacers are covalent assemblies tailored to correlate the cleavage of two chemical bonds in an inactive precursor. The precursor typically contains a protective capping moiety, the central spacer, and the compound of interest. Upon application of an appropriate stimulus, the protective moiety is removed, which generates a cascade of disassembling reactions ultimately leading to release the active compound (Figure 1).

Since their introduction in 1981,^[11–17] self-immolative spacers found applications in prodrugs,^[4,18–32] sensors for chemicals or enzymes,^[33–41] and for drug delivery.^[26–28,30–32,42–46] Self-immolative spacers are also increasingly used in materials science,^[47–51] where their unique feature of kinetically programmable auto-destruction provides unprecedented opportunities for sustainable matter management (i.e. making materials degradable).

For most applications, kinetic information on the disassembly of the activated self-immolative spacer is crucial (e.g.

to control the kinetics of drug release after enzymatic activation or the spatial correlation between the enzyme position and the labeling location; see below). Hence in this Review we report on works addressing kinetic aspects of self-immolation. For users, it will provide the relevant information to guide their choice towards a particular self-immolative motif in relation to a specific demand. Moreover, it will also benefit developers, who will find guidelines to conceive kinetic experiments and exploit the singular kinetic features of self-immolative spacers.

The Review is organized as follows. It first introduces the two main currently used self-immolation processes for which the key step is elimination via electronic delocalization or cyclization. Then the major factors are detailed for analyzing the mechanism and the kinetics of self-immolation processes. The third and fourth sections dissect the significance of the precursor structure on its self-immolation kinetics. They also report on the role of control parameters, such as solvent,

From the Contents

1. Introduction	7493
2. Self-Immolative Processes	7494
3. Kinetic Analysis of Self-Immolation	7495
4. Structure–Property Relationships	7497
5. Kinetics in Action	7503
6. Conclusion	7507

[*] Dr. A. Alouane, Dr. T. Le Saux, Prof. Dr. L. Jullien
Ecole Normale Supérieure–PSL Research University
Department of Chemistry, 24, rue Lhomond, 75005 Paris (France)
E-mail: Ludovic.Jullien@ens.fr

Dr. A. Alouane, Dr. T. Le Saux, Prof. Dr. L. Jullien
Sorbonne Universités, UPMC Univ Paris 06, PASTEUR
75005 Paris (France)

Dr. A. Alouane, Dr. T. Le Saux, Prof. Dr. L. Jullien
CNRS, UMR 8640 PASTEUR, 75005 Paris (France)

Dr. A. Alouane, Dr. F. Schmidt
Institut Curie, Centre de Recherche
26, rue d'Ulm, 75248 Paris (France)
E-mail: Frederic.Schmidt@curie.fr

Dr. A. Alouane, Dr. F. Schmidt
CNRS, UMR 3666, 75248 Paris (France)

Dr. A. Alouane, Dr. F. Schmidt
INSERM, U 1143, 75248 Paris (France)

Dr. R. Labruère
Institut de Chimie Moléculaire et des Matériaux d'Orsay
UMR CNRS 8182, Université Paris Sud, 91405 Orsay Cedex (France)

Supporting information for this article is available on the WWW under <http://dx.doi.org/10.1002/anie.201500088>.



Figure 1. Schematic representation of a self-immolative spacer. The cleavage of Bond 1, which links a protecting group (PG) to the spacer, spontaneously causes the cleavage of the Bond 2, linking the spacer to the desired compound (shown as an ellipse). Thus a primary activating event disassembles the initial precursor into three moieties.

pH value, or temperature. The final section deals with kinetic considerations for tailoring a self-immolative spacer to fulfil a targeted molecular function.

2. Self-Immolative Processes

Self-immolation is governed by the structure of the spacer. Two self-immolative processes have gained wide acceptance. In the first process, the liberation of the desired compound results from an electronic cascade leading to the formation of a quinone or azaquinone methide intermediate. In the second process, spacer disassembly involves a cyclization giving for

instance imidazolidinone, oxazolidinone, or 1,3-oxathiolan-2-one ring structures. In both cases, precursor activation generates nucleophilic functional groups, such as hydroxy, amino, or thio groups, conjugated with or near a leaving group, their reaction spontaneously activates the self-immolation process releasing the desired compound.

2.1. Self-Immolation by 1,4-, 1,6-, or 1,8-Elimination

Self-immolative spacers relying on an electronic cascade for disassembly contain an aromatic structure bearing a hydroxy,^[52–54] an amino,^[55,56] or a thiol,^[19] group. As long as they



Ahmed Alouane is interested in developing chemical tools for biological/medical applications. During his Ph.D. work, he examined a series of aromatic self-immolative spacers to extract structure-property relationships with respect to the kinetics of the self-immolation step.



Frédéric Schmidt is Senior Scientist (Directeur de Recherche) at the CNRS and team leader in chemistry at the Institut Curie (Paris). His research interests are mainly targeting strategies for antitumor agents, chemistry of antitumor agents, self-immolative spacers, bioconjugation (protein coupling techniques), chemical biology of cell membranes, and kinase inhibitors.



Raphaël Labruère is an assistant professor of bioorganic chemistry at Université Paris Sud. Over the last ten years, he gained experience in the development of small-molecule therapeutics and self-immolative spacers constructs as new tools in quantitative biology. His current research focuses on the development of stimuli-responsive biological effectors containing a self-immolative spacer.



Ludovic Jullien is professor of chemistry at Université Pierre et Marie Curie (Paris) and member of the group of biophysical chemistry at Ecole Normale Supérieure (Paris). He has developed various tools for quantitative dynamic descriptions in biology with emphasis on light to perturb and to read-out.



Thomas Le Saux is an assistant professor of analytical chemistry at Université Pierre et Marie Curie (Paris) and member of the group of biophysical chemistry at Ecole Normale Supérieure (Paris). His research interests deal with the development of instruments and methodologies relying on reactivity to perform highly selective chemical analysis.

are protected (or masked), these functional groups are not nucleophilic enough to trigger the process of electronic delocalization in the non-activated precursor. However, activation by an external stimulus reveals their intrinsic nucleophilicity and initiates the self-immolation liberating the desired compound after one or several steps (Figure 2).

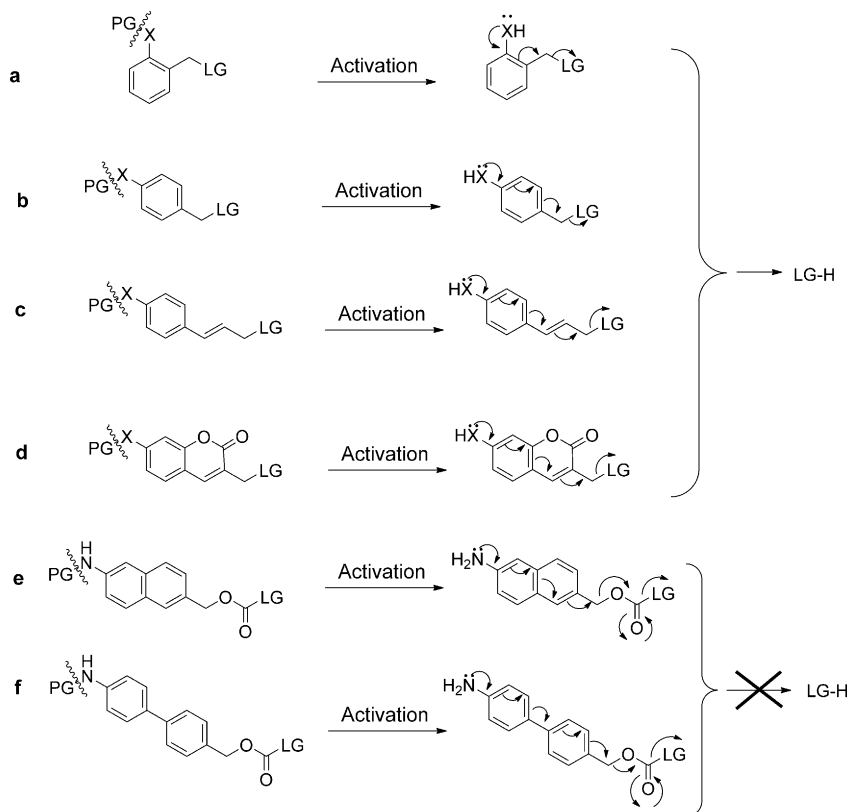


Figure 2. Self-immolative spacers relying on an electronic cascade (*ortho* or *para* delocalization) for disassembly. PG = protecting group; X = O, NH, or S; LG = leaving group belonging to the desired compound. a) 1,4-elimination;^[52–54, 71] b) 1,6-elimination;^[52, 54, 55, 71] c), d) 1,8-elimination;^[44, 56, 57] 1,8-elimination involving a naphthalene ring (e) or 1,10-elimination involving a biphenyl (f) do not occur, even with a strongly donating amino group.^[58]

Driven by its positive entropy and the formation of stable products (e.g. CO₂ when carbonates or carbamates are included in the spacer), self-immolation by electron delocalization occurs both spontaneously and irreversibly.

To date, most reported self-immolative spacers in this series rely on 1,4- (Figure 2 a) or 1,6- (Figure 2 b) eliminations. 1,8-elimination was shown to be possible in *para*-amino(or hydroxy)cinnamyl alcohol (Figure 2 c) or coumarinyl alcohol (Figure 2 d) spacers.^[44, 56, 57] In contrast, putative self-immolative spacers based on combinations of contiguous (such as naphthalene for 1,8-elimination; Figure 2 e) or successive (like in biphenyl for 1,10-elimination; Figure 2 f) aromatic rings do not lead to release the leaving group. This phenomenon has been tentatively explained by too high an energy barrier to break aromaticity and by repulsion of hydrogen atoms in the *ortho* position of biphenyl that prevents the planar structure required for good electron delocalization.^[58]

2.2. Self-Immolation by Cyclization

Self-immolative spacers exploiting cyclization for their disassembly, incorporate linkers based on alkyl chains (Figure 3 a,b),^[15, 59–63] or on *ortho* mono- or disubstituted aromatic spacers (Figure 3 c–e).^[62, 64–70] Once activated, their disassembly involves a nucleophilic attack on a carbonyl group (Figure 3 a–d) or an electrophilic aliphatic carbon atom (Figure 3 e).^[68] The associated cyclization occurs directly after activation or after a preliminary elimination step (Figure 3 b).^[59] As with electronic delocalization, self-immolation is driven by a positive reaction entropy and by the formation of thermodynamically stable products (5- and 6-membered rings).

3. Kinetic Analysis of Self-Immolation

To analyze the mechanism of self-immolation and its rate constants, requires choosing a triggering action and monitoring the formation of the desired compound (and possibly intermediates).

3.1. Self-Immolation: A Multistep Process

Most experiments aiming at analyzing the kinetics of disassembly of an activated self-immolative spacer rely on measuring the temporal evolution of the concentration in the desired compound after the activation of the precursor is triggered. Focusing on the species which contain the desired compound, the complete mechanism is a series of irreversible unimolecular reactions (Figure 4).^[52–54] When their rate constants are different, the concentrations of the precursor, the intermediates, and the released compound evolve multi-exponentially with as many relaxation times τ_i as rate constants k_i (with $\tau_i = 1/k_i$).^[72] However, the temporal resolution of the kinetic experiment governs the number of relaxation times (and thus rate constants), which can be effectively extracted from the observables. Indeed, any reaction occurring faster than the temporal resolution “vanishes” from the temporal system response.^[53, 73]

To analyze self-immolation, a key parameter is therefore temporal resolution.^[74, 75] It depends on two main factors. Temporal control over the initial time of the kinetic experiment is the first. For instance, to rely on mixing the content of a cuvette (which typically requires a second for stirring) to achieve precursor activation only allows access to rate constants smaller than 1 s^{−1} in the disassembly mechanism. In contrast, to turn on light for triggering disassembly of a photoactivatable self-immolative spacer can permit rate constants up to 10⁴ s^{−1} to be measured. The other key factor

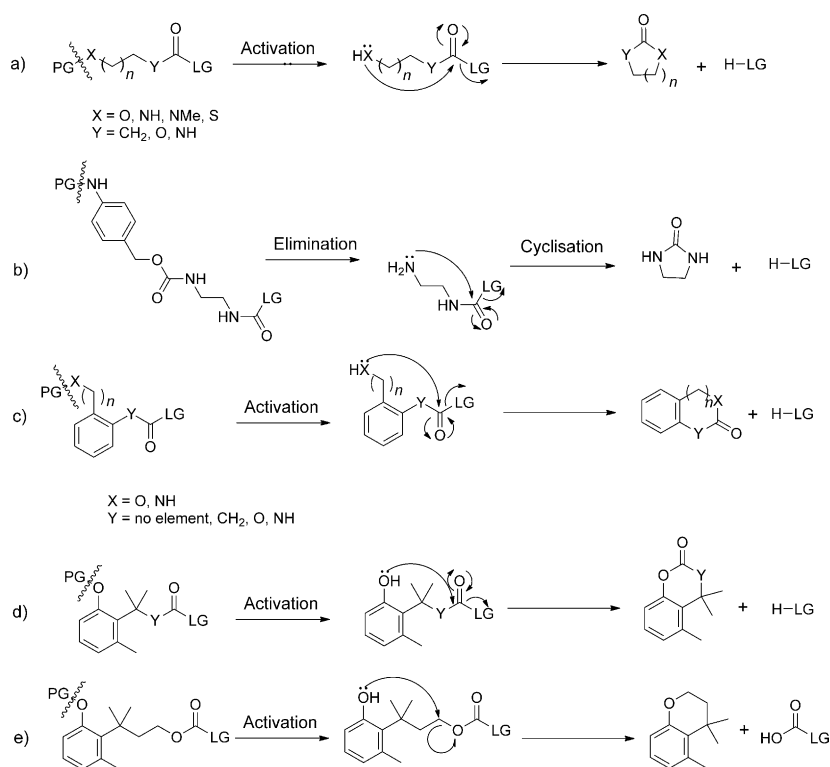


Figure 3. a)–e) Self-immolative spacers relying on a 1,5- or 1,6-cyclization for disassembly. PG = protecting group; LG = leaving group belonging to the desired compound.

controlling temporal resolution is the acquisition frequency during the kinetic experiment: it is not possible to access any rate constant, which is larger than the acquisition frequency. Hence, it is more favorable to collect *in situ* a sensitive observable to exhaustively report on a disassembly process, since it allows the kinetic experiment to be performed at high acquisition frequency. Although relying on HPLC analysis to follow self-immolation is relevant to analyze rate constants below the min⁻¹ range, monitoring the emission from a fluorescent reporter *in situ* will easily give access to rate constants as high as 10³ s⁻¹.

For instance, the last step (proton exchange) of the overall mechanism shown in Figure 4a is so fast (typically submicrosecond time scale) that it has not been accessible in any reported kinetic experiments: the dynamic response of the self-immolative spacer has been reliably modelled as a two-step process, with the two rate constants (*k*₁ and *k*₂) being associated with the cleavage of the protecting group (activation) and the release of the leaving group (self-immolation), respectively.^[53] An additional step associated with a rate constant *k*₃ may have to be considered to model self-immolation when it involves decarboxylation of carbonates or carbamates,^[53] or elimination from a tetrahedral intermediate (Figure 4b,c). Notably for the decarboxylation of carbonates or carbamates, this step occurs on the millisecond time scale under mildly basic conditions at room temperature for the carbonates and at physiological temperature for the carbamates.^[53,54] Under these conditions its rate constant is large enough for the three step model to dynamically decrease to a two steps model.

Note, we assumed above that only the species containing the desired compound could be observed in the kinetic experiments. However, other reactions may take place during the self-immolation process. Hence, in the course of spacer disassembly by electron delocalization, a reactive by-product intermediate quinone methide (for self-immolative phenols) or azaquinone methide (for self-immolative anilines) is released and rapidly attacked (millisecond time scale) by nucleophiles or protic polar solvents.^[76]

3.2. Triggering the Activation of Self-Immolation

The first step of the self-immolation process involves a trigger, which leads to removal of a protecting moiety and liberation of the nucleophilic functional group initiating spacer disassembly. Currently more than 20 trigger/protecting moiety combinations responding to various criteria (such as activation rate, reporting observable, but also solubility and stability of the precursor) have been used in kinetic experiments performed *in vitro* as well as *in vivo*.

Herein they are reported according to the nature of the trigger: a chemical reagent, an enzyme, or light (Tables 1–3).

3.2.1. Activation by Chemical Reagents

Because of its ease of introduction and cleavage, chemical activation mediated by electron exchange, nucleophilic attack, or proton exchange was the first developed to trigger self-immolation.

Activation reactions relying on electron exchange have been mostly achieved by transition-metal-containing reagents or thiols (reductions), and H₂O₂ (oxidation). Treated under mild conditions with zinc/acetic acid, the nitro group yields an amine, which initiates self-immolation (entry 1, Table 1).^[56,77–79] Note, this mode of activation can also be triggered by enzymes (see below). The allyloxy and allylamino groups have been activated by metal-containing reducing agents, such as [Pd(PPh₃)₄]/NaBH₄, [Pd(PPh₃)₄]/(Bu)₃SnH, [PdCl₂(PPh₃)₂]/KBH₄ (entry 2, Table 1).^[80–86] In particular, the allyloxy group has been used to release a hemiacetal that subsequently decomposed into a dialdehyde.^[83] Disulfide bridges provide biologically relevant precursors to initiate self-immolation after activation by thiols,^[87] such as dithiothreitol^[32,88] (entries 3–4, Table 1). Phenylboronates have been activated by hydrogen peroxide (entry 5, Table 1).^[49,89–93] In particular, this system has been used in prodrugs of matrix metalloproteinase inhibitors.^[94]

The second class of chemical activators relies on a nucleophilic attack to initiate self-immolation. Silylated ethers have been activated by the fluoride anion (entry 6,

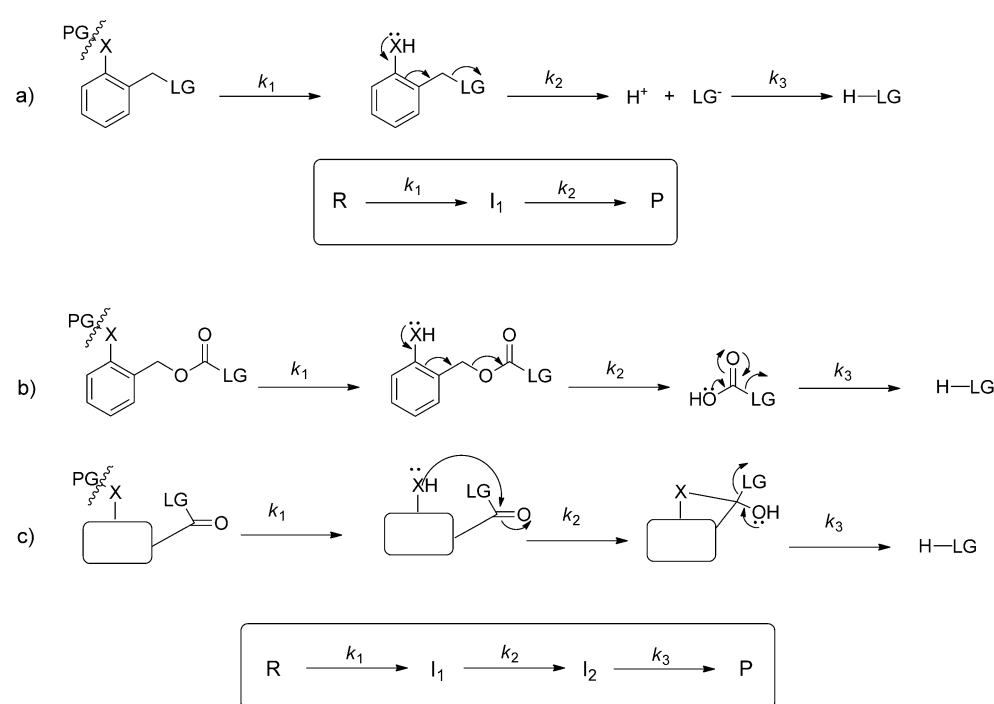


Table 1).^[52,83,95] Water was used to cleave labile esters (entry 7, Table 1),^[59] which enabled slow activation under physiological conditions.

Activation reactions based on proton exchange have mainly involved Boc^[57,59,60,96–100] and Fmoc^[98] carbamate protecting groups of amines. After activation, decarboxylation takes place before liberation of the desired compound (entries 8–10, Table 1).

3.2.2. Enzymatic Activation

Self-immolative spacers have become increasingly popular in prodrug strategies after developing various triggering methods *in vivo*, such as enzymatic activations. For kinetic experiments, enzymatic activations are generally rather slow.

Plasmin-induced cleavage of a tripeptide enabled the release of drugs with a 1,6-elimination spacer^[58] (entry 1, Table 2). Enzyme activation proved to be highly sensitive to steric hindrance: The half-life associated with enzymatic activation by plasmin dropped from 42 to 4 min when the activation was combined with the cyclization of *N,N'*-ethylenediamine. Antibody 38C2-mediated activation by a retroaldol retro-Michael reaction has been implemented to liberate drugs or 4-nitrophenol (entry 2, Table 2).^[42,45,100–103] Penicillin G amidase (PGA) and Bovine Serum Albumin (BSA) have been used to cleave the phenylacetamide moiety

(entry 3, Table 2)^[34,38,44,45,55,92,96,99,100,104–108] and a carbamate^[109] (entry 4, Table 2), and liberate various substrates. β -Glucuronidase (β -GUS)^[33,40,43] (entry 5, Table 2) and β -Galactosidase^[110–112] (entry 6, Table 2) have been successfully implemented to specifically deliver bioactive substrates in tumors and in bacteria.^[110] Eventually a fluorogenic probe containing a self-immolative spacer that was alkaline phosphatase (ALP) sensitive was implemented for the quantitative analysis of ALP activity (entry 7, Table 2).^[113]

3.2.3. Light-Driven Activation

The last protecting moieties discussed in this Review are triggered by light.^[114] From the point of view of kinetic analysis, they benefit from not requiring a mixing step to stimulate their cleavage (see above).

The photolabile *o*-nitrobenzyl group is activated by UV illumination,^[53,54,63,73,97,115–118] which causes its cleavage in less than 1 ms when good leaving groups are released^[53,54,73] (entry 1, Table 3). In particular, this time scale yields an excellent temporal resolution to analyze fast self-immolations^[53,54,73] by using fluorescent reporters. Interestingly the cleavage of the bromocoumarin caging group (entry 2, Table 3) has been carried out by irradiation in the near infra-red (NIR) wavelength range^[63,119] to trigger the degradation of long polymers and nanoparticle spheres containing self-immolative spacers.

4. Structure–Property Relationships

As an outcome of the kinetic analysis, the basic principles of which have been introduced above, this Section dissects the significance of the precursor structure on its self-immolation kinetics for both spacers based on elimination by electronic cascade and by cyclization. It also shows the role of control parameters, such as solvent, pH value, or temperature.

Numerical data in Tables 1S–7S (see Supporting Information) give rate constants and half-times for the compounds 1–110 shown in Figure 5–11. It should be emphasized that most of the publications analyzed report only apparent rate constants *k* and disassembly half-times *t*_{1/2} and not an

Table 1: Kinetic analysis of self-immolation after chemical activation.^[a]

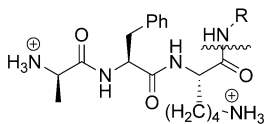
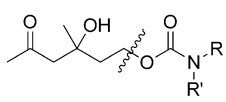
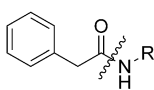
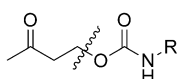
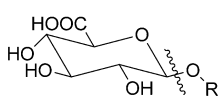
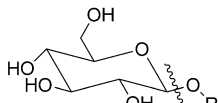
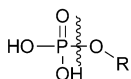
Entry	Protecting group	Trigger	Reporting molecule	Anal. tool	Ref.
1		Zn/AcOH Zn/AcOH Radiolytic reduction	Paclitaxel Tryptamine Hydroxylamines	N H H	[56] [77] [78, 79]
2		[Pd(PPh ₃) ₄]/NaBH ₄ ; [PdCl ₂ (PPh ₃) ₂]/KBH ₄ [Pd(PPh ₃) ₄] [Pd(PPh ₃) ₄]/NaBH ₄ [Pd(PPh ₃) ₄]/[(t-Bu) ₃ SnH]	<i>p</i> -Nitrophenol <i>o</i> -Phthalaldehyde 2,4-Dimethylphenol Substituted phenols	U G, N N U	[80, 82] [83] [84] [85, 86]
3		Dithiothreitol	Epothilone Paclitaxel, daunomycin	H H	[88] [32]
4		Thiols	BODIPY	U, F	[87]
5		H ₂ O ₂	Alcohols Arenes 4-Nitroaniline Fluorescent aniline Fluorescein, Fluorescent reporter 5-Amino-2-nitrobenzoic acid 7-Hydroxycoumarin Hydroxylamines, Enols	N U U H F U F U	[89] [90] [91] [49] [92] [93] [93] [94]
6		Fluoride	7-Hydroxycoumarin <i>o</i> -Phthalaldehyde 4-Nitroaniline	F G U	[52] [83] [95]
7		H ₂ O	4-Hydroxybenzylalcohol Nile Red	N F	[59] [59]
8		TFA	Aminomethylpyrene 4-Hydroxybenzylalcohol 6-Aminoquinoline Aminomethylpyrene, 4-Nitroaniline Polymer Phenol	F, H N F H G U	[57] [59] [96] [97] [98] [60]
9		Piperidine Morpholine	4-Nitroaniline, 1-Naphthylamine 4-Nitroaniline	H U	[99] [100]
10		Piperidine	Azaquinone methide	G	[98]

[a] The columns 1–5 respectively indicate the entry number, the protecting group with the position of cleavage, the chemical trigger, the released substrate, and the tool for kinetic analysis of substrate release: N = NMR, H = HPLC, U = UV/Vis, G = GPC, F = Fluorescence.

exhaustive set of rate constants (and relaxation times), including the one specifically associated with the self-immolation step (see above). Therefore, upon considering that the rate-limiting step in precursor disassembly may be activation not self-immolation, comparison between data acquired with

various activation modes should be performed with care. Hence it is more reliable to perform kinetic analysis on homogeneous sets of data obtained with the same type of activation and under the same experimental conditions.

Table 2: Kinetic analysis of self-immolation after enzymatic activation.^[a]

Entry	Protecting group	Trigger	Reporting molecule	Anal. tool	Ref.
1		Plasmin	Doxorubicin, paclitaxel	H	[58]
2		Catalytic antibody 38C2 (Ab38C2)	Doxorubicin, camptothecin Etoposide 4-Nitrophenol Ab38C2	C H U F	[42, 101, 103] [102] [45] [100]
3		Penicillin-G-amidase (PGA)	7-Hydroxycoumarin Melphalan 4-Nitrophenol Doxorubicin 6-Aminoquinoline 4-Nitroaniline 5-Amino-2-nitrobenzoic acid 1-Naphthylamine Tryptophane Cy5 Fluorescent reporters Camptothecin PGA	F F, H U H U, F H H H H F F H F	[34, 38] [44, 105] [45, 106] [45] [96, 106] [55, 99] [55, 108] [99] [105] [92] [38, 104, 107] [107] [100]
4		BSA	4-Nitroaniline Fluorescent Amine	H F	[109] [109]
5		β -Glucuronidase	4-Hydroxy-3-nitrobenzyl alcohol 2SBPO Doxorubicin	U F H	[33] [40] [43]
6		β -Galactosidase	Glucose SulfoQCy7 Doxorubicin Monomethyl auristatin E	B F H U, H	[110] [110] [111] [112]
7		Alkaline phosphatase	Benzothiazolyl iminocoumarin	F, H	[113]

[a] The columns 1–5 respectively indicate the entry number, the protecting group with the position of cleavage, the enzymatic trigger, the released substrate, and the tool to analyze substrate release: N=NMR, H=HPLC, U=UV/Vis, G=GPC, F=Fluorescence, C=Cell growth inhibition, B=Bacteria growth assay.

4.1. Self-Immolation Based on Elimination by Electronic Cascade

The elimination based on electronic delocalization involves the formation of a quinone or azaquinone methide intermediate and results in loss of electron density at the benzylic position associated with release of a leaving group (see Figure 2). Thus resonance energy of the aromatic ring as well as substituents borne by the aromatic core or at the benzylic position alter the disassembly rate. Furthermore, external parameters, such as the solvent, pH value, or temperature are also anticipated to play a role.

4.1.1. Substituents on the Aromatic Core

An increase in the electron density on the aromatic ring is expected to 1) facilitate dearomatization and 2) assist the cleavage of the bond between the leaving group and the aromatic core by stabilization of the transient positive charge formed at the benzylic position during the elimination leading to the quinone methide intermediate.^[78, 91, 120] In fact, electron-donating groups (e.g. OMe) should increase the energy of the HOMO of the aromatic ring and correspondingly strengthen the HOMO–LUMO interaction between the bonding π ring molecular orbital and the non-bonding σ^* C–LG orbital (LG=leaving group). This interaction should result in the

Table 3: Kinetic analysis of self-immolation after light activation.^[a]

Entry	Protecting group	Trigger	Reporting molecule	Anal. tool	Ref.
1		UV light	<i>p</i> -Nitrophenol	U, N	[115]
			Coumarin	F	[53, 54, 73]
			DDAO	F	[53, 54, 73]
			Nile Red	F	[118]
			Dendrimer degradation	U, G, N	[116]
			Aminomethylpyrene	H	[97]
			Polymer degradation	G, N	[63, 117]
2		NIR light	Polymer degradation	G, N H-M	[63, 119] [119]

[a] The columns 1–5 respectively indicate the entry number, the protecting group with the position of cleavage, the light trigger, the released substrate, and the analytical method to detect the substrate release: N = NMR, H = HPLC, U = UV/Vis, G = GPC, F = Fluorescence.

strengthening of the C–C benzylic σ bond (which becomes shorter) and the weakening of the σ bond C–LG, thus facilitating release of the leaving group. Indeed, the self-immolation rate is significantly accelerated by grafting electron-donating groups (such as, OMe and NHMe; formulas **4**, **7–9**, **12–14**, **18**, **21**, **22**, **26**, **29**, **30**; Figure 5) conjugated or not with the benzylic position^[53, 78, 85, 91, 120] (see Table 1S).

aniline occur at similar rates (formulas **18** and **26**; see Table 1S).

Although the preceding trends seem well-established, it is of note that the same self-immolative spacer (formula **17**) was reported to exhibit two different disassembly half-times: $t_{1/2}$ = 600 s was found with activation by nitro reduction,^[78] whereas $t_{1/2}$ = 17 s was measured when activation was by deprotona-

In contrast, electron-withdrawing substituents induce a drop in electron density on the aromatic ring, which destabilizes the partial positive charge at the benzylic position in the transition state of the spacer disassembly, thus increasing the kinetic stability of the activated spacer. Indeed, self-immolative spacers containing aromatic rings substituted with strong electron-withdrawing functional groups, such as NO₂ (formulas **3**, **6**, **11**) and CO₂Me (formulas **10**, **27**), exhibit a half-life of self-immolation larger than their unsubstituted analogues^[53, 78, 120] (see Table 1S).

As expected from their similar electronic properties in the same ionization state, self-immolations driven either by a phenol or an

X = NH

X = O

	R ² = R ³ = H; R ⁴ = Me				R ³ = R ¹ = H; R ⁴ = Me			R ⁴ = H			R ⁴ = H					
	R ¹	R ²	R ³	R ⁴	R ¹	R ²	R ³	R ¹	R ²	R ³	R ¹	R ²	R ³			
1	H	H	Me	H	6	NO ₂	11	NO ₂	17	H	H	H	25	F	H	H
2	H	Br	Me	Br	7	OMe	12	OMe	18	H	OMe	H	26	H	H	OMe
3	H	H	NO ₂	H	8	NHMe	13	NHMe	19		H					
4	OMe	H	OMe	OMe	9	N(Me)CO ₂ ^t Bu	14	N(Me)CO ₂ ^t Bu								
					10	CO ₂ Me	15	NHOH								
							16	H								

5

20

24

27

21

22

23

28

29

30

tion (see Table 1S).^[121] Such discrepancies may originate from different experimental conditions or rate-limiting steps in the activation–disassembly process.

4.1.2. Aromatic Core

It is important to recognize that the nature of the aromatic core governs the distance between the activation position and the leaving group, independently of any electronic effect. As such, it can contribute to reduce steric hindrance in the case of enzyme activation.^[58,122] The significance of the aromatic core has been further evaluated by reference to resonance energy and electronic effects.

The kinetics of self-immolation were first examined with the benzene ring by analyzing any difference between eliminations involving the benzylic position either *ortho* (1,4-elimination) or *para* (1,6-elimination) to the nucleophilic atom (Figure 2 a,b). In fact, the disassembly times were found to be almost identical for both types of eliminations (formulas **1** and **37**; see Table 1S and 2S respectively).^[52,54,55,71] However, in a system involving dual release, the leaving group located at the *para* position (1,6-elimination) was released faster than the *ortho* one (1,4-elimination).^[55,77] Furthermore, the *para* (1,6-elimination) was also faster than the 1,6-elimination through the vinylogous *ortho*-benzyl position in a spacer involving a dual release.^[99]

The disassembly rate has been also compared in self-immolative spacers containing the benzene aromatic ring and its heteroaromatic analogues. Indeed, upon release of the leaving group by self-immolation, the aromatic ring loses aromaticity. Thus decrease of the resonance energy of the aromatic ring should accelerate the release. Indeed this trend has been observed in the hydrocarbon aromatic series: disassembly of the phenantrene spacer **24** is five-times faster than that of the naphthalene spacer **23**, which is itself 10-times faster than that of the benzene spacer **20** (Table 1S).^[86,91] Pyridine and pyrimidine have a lower resonance energy (142 and 132 kJ mol^{−1}) than benzene (ca. 150 kJ mol^{−1}),^[123] so should be favorable to build fast self-immolative spacers. This was observed in a spacer containing the pyridinic core (formula **31**; Figure 6).^[108] After enzymatic activation, its

self-immolation was complete after 30 min, compared to more than 4 h for the benzenic analogue.^[108] In contrast, other results (see Table 2S) relying on photochemical activation and detailed kinetic analysis demonstrated that the pyridine ring decreases the rate of disassembly relative to the benzene core (see formulas **34** and **37** relatively to others) and that the position of its nitrogen atom is significant (see formulas **31** and **32**). Moreover, it has even been shown that the introduction of two nitrogen atoms in the aromatic core (pyrimidines; formulas **33** and **35**) prevents release of the leaving group under acidic conditions. Thus, more than the drop of the resonance energy, it seems that disassembly kinetics of the heterocyclic self-immolative spacer is controlled by the electron density at the benzylic carbon atom bearing the leaving group. This electron density is lowered by the presence of nitrogen atoms exerting electron-withdrawing effects.

4.1.3. Linking Core Leaving Groups and Substituents at the Benzylic Position

The disassembly half-time of self-immolative spacers is also affected by the link between the aromatic core and the leaving group (see Table 3S). Indeed, half-times larger by several order of magnitudes (> 10³ times)^[52] have been observed for spacers where the leaving group was linked by an ether (formulas **38** and **42**; Figure 7) with respect to analogous spacers in which the leaving group was bound by a carbonate (formulas **39** and **40**) or carbamate (formula **41**).^[52,53] Indeed the carboxylate group is a much better leaving group than the alcoholate group. In fact, the decarboxylation of the carbamic acid may even become rate-limiting in the whole disassembly process: Decarboxylation half-times in the 5 min range have been reported at 293 K.^[53,124] Furthermore, reporters directly linked to the benzylic position through an amine or thiol bond lead to almost no liberation except under rather drastic experimental conditions or specific aromatic substitutions (formulas **27–30**).^[79,90,120]

As expected from the stabilization of the partial positive charge at the benzylic position in the transition state, the introduction of a methyl substituent at the benzylic substituent was also shown to significantly accelerate the elimination of the quinone methide intermediate (compare formulas **44** and **46** with formulas **43** and **45**).^[78,89] A phenyl substituent similarly accelerates the rate of disassembly.^[125]

4.1.4. Leaving Groups

Nucleofugacity governs the last step of self-immolation: it generally increases when the proton exchange constant (pK_a) of the conjugated acid of the leaving group decreases.^[126] This trend has been observed while studying the disassembly kinetics of a family of self-immolative spacers releasing different alcoholates including phenols bearing various substituents (Figure 8 and Table 4S).^[19,85] The disassembly half-life of the spacer was shown to increase exponentially with the pK_a of the free alcohols (formulas **47–50** and formulas **51–53**).

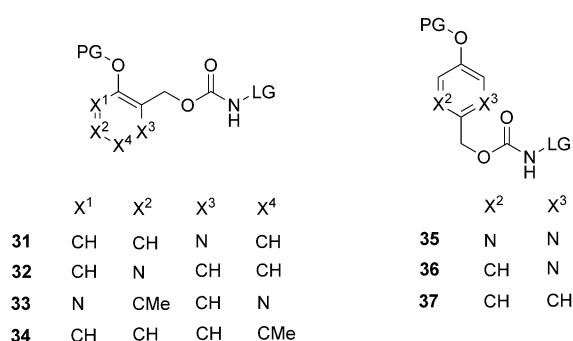


Figure 6. Benzenic and heteroaromatic (pyridine and pyrimidine) rings in self-immolative spacers. The structures on the left and on the right yield *ortho* (1,4-elimination) and *para* (1,6-elimination) release of the leaving group respectively. PG = protecting group; LG-N = leaving group.

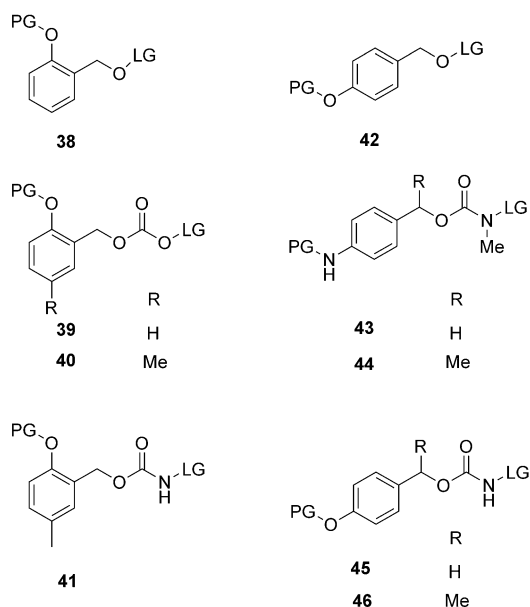


Figure 7. Substrates used to both evaluate the effect of the link between core and leaving group, and the incidents of the substituents at the benzylic position on the rate of elimination caused by electronic delocalization. PG = protecting group; LG-O, LG-N = leaving group.

However, this relationship alone does not account for all the reported behaviors. Hence, in a recent comparative investigation using DDAO and 7-hydroxytrifluoromethyl coumarin (with respective $pK_a \sim 5$ and ~ 7.5 ; formulas **66** and **67**) as leaving groups,^[53] the coumarin was released faster than DDAO. This observation has suggested that conformational effects could also impact the disassembly kinetics and a carbonate linker may decrease the importance of the leaving group's nucleofugacity.^[79]

The significance of the leaving group has been also evaluated in a series in which the activating phenol was generated from oxidation of the arylboronic ester precursors (formulas **54–65**).^[89,90,127,128] Electron-withdrawing groups at

the aromatic ring or benzylic position enhance the rate of arylboronic ester oxidation^[129] but decrease the rate of quinone methide formation. Hence similar rate constants of self-immolation have been reported for formulas **54–59**.^[90,94] Moreover, as expected from sharing a similar carbamate linkage, the compounds **60–64** exhibited essentially similar disassembly half-times.^[89]

4.1.5. Control Parameters

The solvent is anticipated to alter the disassembly rate of activated spacers. Indeed an increase in polarity should stabilize the partial charges, which are developed in the transition state of the self-immolation step. Indeed the disassembly rate in a series of self-immolative spacers involving the formation of quinone methide species increases proportionally with solvent polarity (e.g. H_2O percentage in a $H_2O/MeCN$ mixture).^[85]

As strikingly evidenced in self-immolative spacers containing a phenol core, pH value also controls the disassembly rate by means of the ionization state of the nucleophilic atom liberated after removal of the capping protecting group. Hence phenol ionization accelerates the disassembly rate by a factor 100 over the 4–10 pH range (formulas **2** and **3** with respective phenol pK_a 9.5 and 8.1).^[53] The pH effect was even more pronounced for pyrimidine-containing spacers (see formulas **33** and **35**) since disassembly of the activated precursor could be launched when increasing pH value from 4 to 9.5.

Temperature was also shown to affect the rate of self-immolation: a ten-fold increase of the disassembly rate was observed upon increasing temperature from 293 K to 318 K.^[53]

4.2. Self-Immolation Based on Cyclization

The cyclization strategy has been applied in pro-drugs,^[4,18–25,130–134] sensors,^[34–36,38,41] and drug delivery sys-

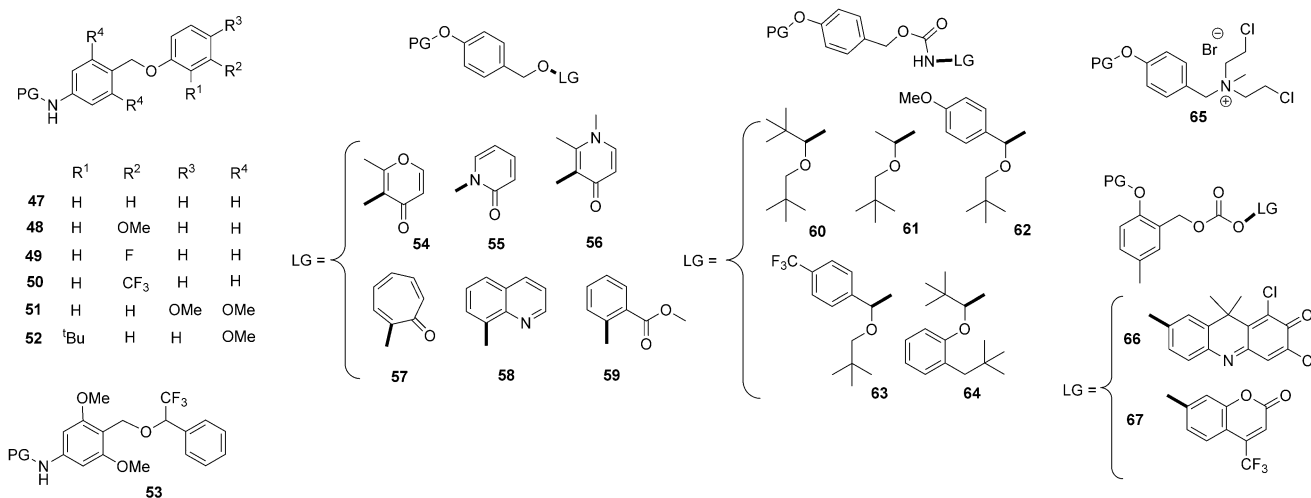


Figure 8. Substrates used to evaluate the effect of the leaving group on the rate of elimination caused by electronic delocalization. PG = protecting group; LG-O, LG-N = leaving group.

tems.^[26–28,30,32,88] Disassembly of self-immolative spacers based on intramolecular 5-*exo*-trig or 6-*exo*-trig cyclization yields cyclic esters, ureas, carbamates, or thiocarbonates^[59,63] (Figure 3a–c). In most cases, cyclization occurs more slowly than elimination by electronic cascade. When cyclization is combined with 1,6-elimination (Figure 3b), it is often the rate-limiting step.^[63,105] However, this combination is useful to facilitate enzymatic activation by lowering steric hindrance or providing chemically stable precursors (e.g. engaging an alcohol in a carbamate).

In contrast to the preceding series, the kinetics of cyclization-driven disassembly are mainly governed by conformational aspects (Thorpe–Ingold effect^[63,105] and/or reactive rotamer effect).^[135] However, the electrophilicity and nucleophilicity of the sites involved in the cyclization also bring significant changes on the half-time of self-immolation by cyclization.

4.2.1. Substituents on the Spacer

Substituents differing by their size and their electronic effects have been introduced in the α position of the ester function of linear alkyl spacers (Figure 9) to examine the Thorpe–Ingold effect^[63,105] and/or the reactive rotamer effect^[135] on the kinetics of cyclization. Half-times of cyclization ranged between 2 and 39 s at pH 7.4 and 37 °C (Table 5S).^[60]

Introducing a methyl group on the amino group of the spacer (formula **69**) accelerated cyclization by a factor of 4. Furthermore, as expected by the Thorpe–Ingold^[42,58] and reactive rotameric effects,^[101] mono (formulas **70**, **74**, **75**) and di- (formulas **71** and **72**) substitutions in the α position of the ester induced similar accelerations of the cyclization. Such conclusions have been also supported by the “trimethyl lock” effect.^[67] However, the insertion of two benzylic substituents (formula **76**) in the same position decreased the rate of cyclization by a factor of 4 with respect to the other substituents. In contrast, engaging both α positions in a cyclopentyl ring yielded a much shorter half-life of the activated spacer (formula **78**). Finally, the introduction of hydroxy

groups (formulas **73** and **77**) accelerated the cyclization more effectively than all the other substituents.

The significance of substituents was also shown in the series in Figure 10.^[136] After bioreduction of the nitro group, these 2-aminoaryl amides release their substrate after spontaneous cyclization by the nucleophilic attack of the aniline generated on the carbonyl of the amide bearing the leaving group. Cyclization rates at pH 2.4 varied by more than a factor 50 000 (Table 6S), revealing the significance of substituents in the spacer (formulas **91**, **92**, and **97**), at the benzylic position (formulas **79–84**) but also on the amino leaving group (formulas **81** and **82**).

4.2.2. Electrophilicity and Nucleophilicity of the Sites Involved in the Cyclization

Tuning the electrophilicity and nucleophilicity of the sites involved is relevant to alter the rate of the cyclization reaction. Hence, replacing an electrophilic carbamate site with a carbonate decreased the cyclization half-life of the spacer 500-fold. The self-immolation rate was further increased by replacing the nucleophilic amine with a thiol.^[137]

As in the preceding series of self-immolative spacers acting by elimination, there is a correlation between the pK_a value of the leaving group and the rate constant of spacer disassembly. This correlation has been evidenced in a series of thioamides^[138] (Figure 11 and Table 7S): *para*-electron-donating substituents, such as OMe and Me (formulas **104** and **105**), increase the pK_a value of the leaving phenol and lower the cyclization rate by several orders of magnitude with respect to leaving phenols containing strongly electron-withdrawing groups, such as NO₂ (formula **110**).

4.2.3. Control Parameters

The pH value exerts a significant impact on the rate of self-immolation by cyclization when a pH-sensitive group is liberated after spacer activation. Hence, for 4-aminobutyric acid containing spacers, the self-immolation rate of the compound **78** is fastest at pH 7.4 but drops when the pH value decreases to pH 4.

5. Kinetics in Action

After the many attractive features presented above, this Section now elaborates on the kinetic opportunities provided by self-immolative spacers to liberate a product after activation. The simplest kinetic scheme (subsequently denoted as **RP**): one-step product **P** liberation after precursor **R** activation (Figure 12a) is used as a reference behavior. The temporal evolutions of the precursor and product concentration are first examined when the system is homogeneous. We subsequently address the case of localized activation, which is relevant for prodrug applications where a drug is expected to be liberated in the neighborhood of activating markers (e.g. enzymes). We end up with an examination of self-immolative spacers releasing several products after activation.

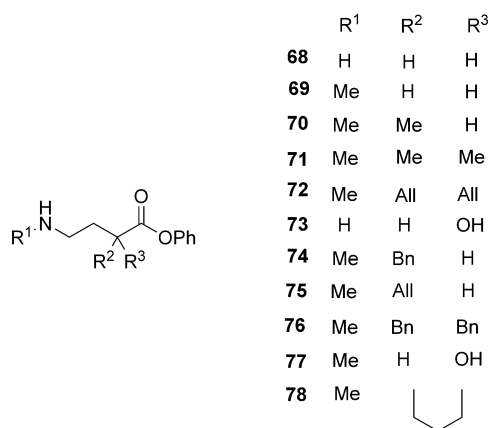


Figure 9. Substrates used to evaluate the effect of the substituents at the α position of the linear spacers on the rate of elimination by cyclization.

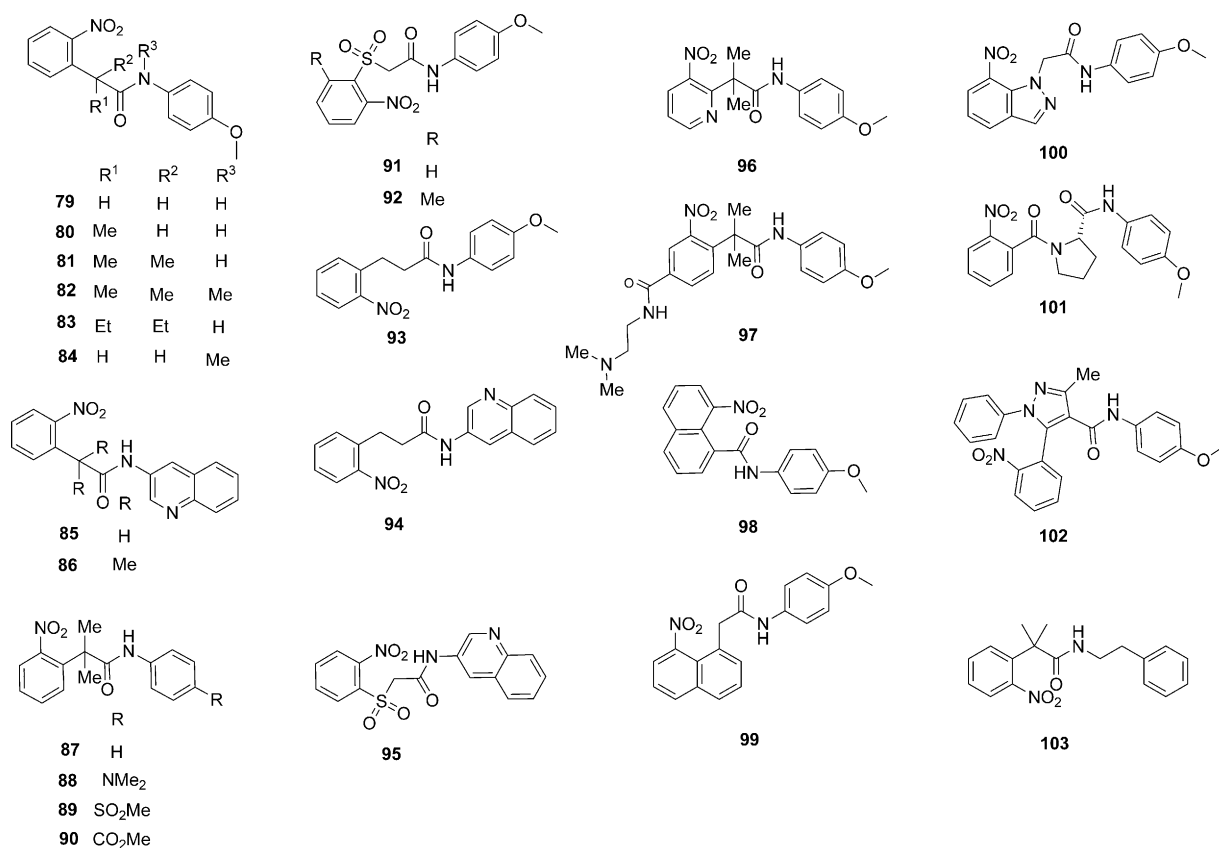


Figure 10. Substrates used to evaluate the effect of the substituents in the spacer on the rate of elimination by cyclization.^[136]

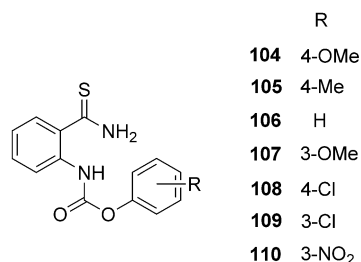


Figure 11. Substrates used to evaluate the effect of the leaving group on the rate of elimination by cyclization.

5.1. Temporal Control of Product Liberation

Although disassembly of a self-immolative spacer may involve multiple steps, it is relevant in the following discussion to adopt the simple dynamic model (subsequently denoted as **RIP**) shown in Figure 12b, which involves two irreversible unimolecular steps: activation of the precursor **R** to yield an intermediate **I** and subsequent rate-limiting step leading to product liberation.^[53,73]

Figure 13 displays the simulated temporal evolution of the concentrations in the non-activated precursor **R**, the activated self-immolative spacer **I**, and the desired product **P** when activation occurs in a closed homogeneous system with different values for the rate constants associated with the

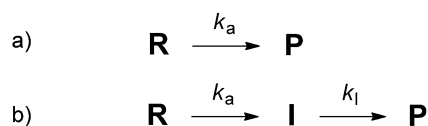


Figure 12. The **RP** (a) and the **RIP** (b) kinetic model.

activation (k_a) and liberation (k_i) steps. For comparison, Figure 13 also shows the corresponding temporal evolutions for the non-activated precursor **R** and the product **P**, when product liberation directly occurs after **R** activation.

With respect to direct product liberation after **R** activation, Figure 13 emphasizes the key opportunities provided by self-immolative spacers for product liberation. Whereas the temporal evolution of the non-activated precursor is identical for both dynamic models, product liberation occurs after a delay τ_a when a self-immolative precursor is used. However, to observe this delay requires that product liberation is slower than precursor activation ($k_i < k_a$) (in the opposite case, i.e. $k_i > k_a$, both **RIP** and **RP** dynamic models do not differ), which can be achieved by an appropriate choice of the self-immolative motif. Note that the concentration of the intermediate **I** is only significant in the $k_i < k_a$ case (otherwise its concentration is vanishing) between the times τ_a and $\tau_i = 1/k_i$. This last point is particularly relevant for the design of efficient self-immolative precursors transiently generating trapping quinone methide intermediates for DNA alkylation

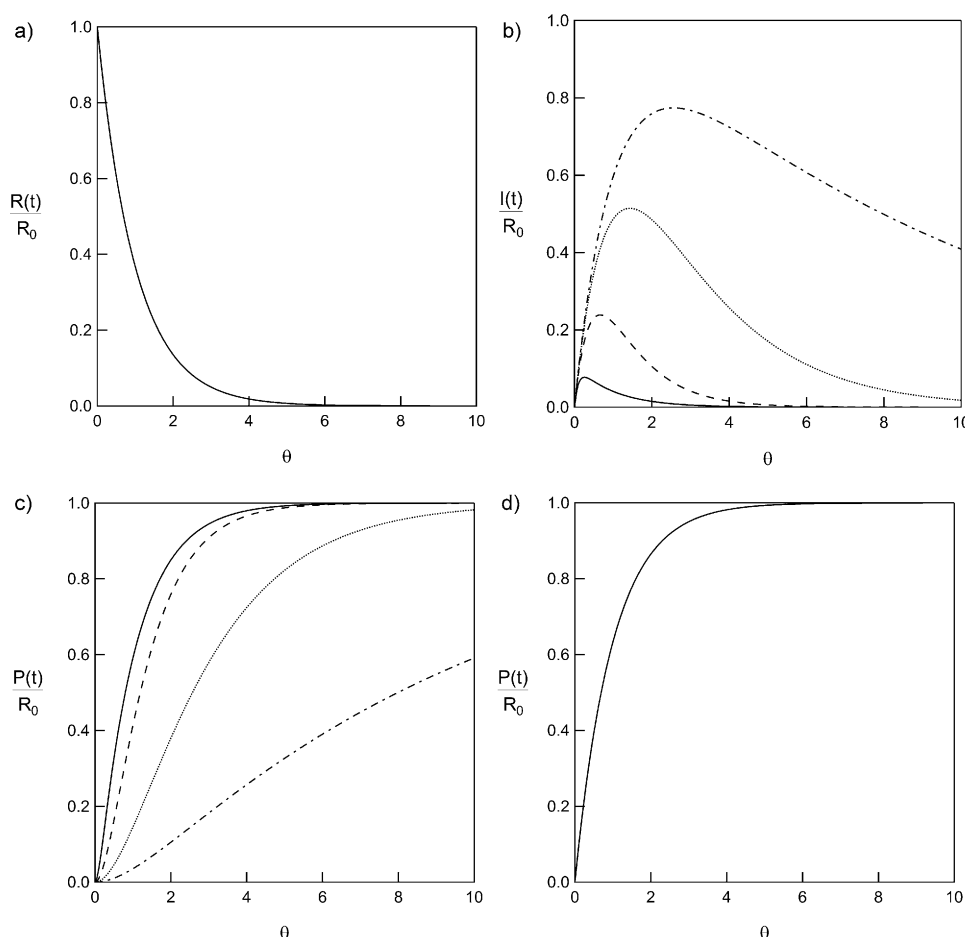


Figure 13. Temporal evolution of the concentrations in the non-activated precursor **R** (a), the activated self-immulative spacer **I** (b), and the desired product **P** (c,d) (normalized to the initial concentration R_0 of the non-activated precursor) associated to the dynamic models shown in Figure 12b: a)–c) $R(t)/R_0 = \exp(-k_a t)$, $I(t)/R_0 = [k_a/(k_1 - k_a)][(\exp(-k_a t) - \exp(-k_1 t))]$, $P(t)/R_0 = 1 - [k_1 \exp(-k_a t) - k_a \exp(-k_1 t)]/(k_1 - k_a)$, and Figure 12a: a), d) $R(t)/R_0 = \exp(-k_a t)$, $P(t)/R_0 = 1 - \exp(-k_a t)$. $\theta = t/\tau_a$ ($\tau_a = 1/k_a$) is the time variable in the plots. For the **RIP** dynamic model, the temporal evolution has been plotted for the following values of the ratio k_1/k_2 : 0.1 (dashed-dotted line), 0.46 (dotted line), 2.15 (dashed line), 10 (solid line). See References [53, 73] for the derivation of the kinetic equations.

(Figure 14).^[139–142] In this strategy, the substituents of the benzenic core of the spacer have been modified to optimize alkylating properties.^[142]

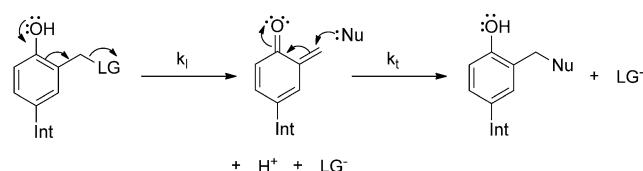


Figure 14. Self-immolation for generating trapping species for DNA alkylation. The relative values of the rate constants associated to self-immolation (k_i) and to nucleophile trapping by the quinone methide intermediate (k_t) permit tuning both the maximum concentration of the trapping species and the kinetic window in which it survives. LG = Leaving group; Int = Intercalating moiety; Nu = Nucleophile belonging to DNA.

5.2. Spatial Control of Product Liberation

When the system is not closed, molecular motion affects the concentration profiles. In relation to prodrug applications, which have significantly motivated the development of self-immulative systems, the case of localized activation (e.g. by enzymatic activation) is specifically examined. Two different situations are successively considered: 1) activation occurs in an open system, as in prodrug strategies, such as antibody-directed enzyme prodrug therapy (ADEPT)^[143] in which precursor activation occurs at cellular surfaces with subsequent local internalization of the liberated drug; 2) intracellular prodrug activation and drug liberation, which is relevant of therapeutic approaches like gene-directed enzyme prodrug therapy (GDEPT).^[144]

Following the derivation provided in the literature,^[145] activation of the self-immulative spacer is considered to occur in a sphere of radius r located in an infinite medium containing a reservoir of freely diffusing non-activated precursor **R** with concentration R_0 . For simplification, all the species **R**, **I**, and **P** are supposed to

share a same diffusion coefficient D . Then the diffusion time $\tau_d = r^2/D$ typically evaluates the time to enter the sphere volume by diffusion.^[145] When product liberation directly occurs after precursor activation (**RP** model), the steady-state **P** concentration is at the highest within the activation sphere (out of the sphere, it decays as the inverse of the distance from its center): it is equal to R_0 when $\tau_a < \tau_d$ and scales as $(\tau_d/\tau_a)R_0$ when $\tau_a > \tau_d$.^[145] Taking $r = 100 \mu\text{m}$ (a few cells in diameter) and $D = 10^{-10} \text{m}^2 \text{s}^{-1}$ (typical for a molecule of medicinal interest) yields 100 s as an order of magnitude for τ_d . Thus activation should typically occur faster than in 100 s to locally deliver the desired product **P** at the nominal R_0 concentration. When using a self-immulative spacer (**RIP** model), the same result now requires both $\tau_a < \tau_d$ and $\tau_1 < \tau_d$ to be fulfilled.^[145] Hence, to co-localize product liberation with precursor activation at the concentration of the non-activated precursor (a much sought after goal in the prodrug design) is kinetically constrained: the fastest activation and self-immulative chemistry must be chosen.

Activation of the self-immolative spacer is subsequently considered to occur in a small volume circumvented by a permeable shell (a crude model for a cell) such that the intra-sphere concentration of the non-activated precursor **R** is maintained constant at R_0 by contact with the infinite external reservoir.^[145] Instead of a diffusion time, it is now a permeation time τ_p , which will affect the concentration profiles. For the steady-state **P** concentration to be equal to R_0 necessitates $\tau_a < \tau_p$ (**RP** model) and both $\tau_a < \tau_d$ and $\tau_1 < \tau_d$ (**RIP** model). Again fast activation and self-immolative chemistry are favorable to achieve co-localization of the product liberation with precursor activation at the concentration of the non-activated precursor.

In particular, the preceding reasoning is relevant in analyzing the behavior of prodrugs based on the reduction of 4-nitrobenzyl carbamates for the release of alkylating agents in a nitroreductase GDEPT strategy.^[146,147] In vitro the faster prodrugs bearing electron-donating substituents on the nitrobenzyl core ensured a better selectivity toward cancer cells expressing the nitroreductase than to healthy cells.^[147] This reasoning also accounts for the enhanced rate of disassembly of a self-immolative-based profluorophore probe improving the enzymatic detection in the sensing and cellular imaging of human cancer enzyme.^[148]

5.3. Liberation of Multiple Products

The case of a non-active precursor releasing multiple products after its activation can be considered. In this Review, the situation is restricted to one in which two products, **P**₁ and **P**₂, are liberated.^[53,73] For the following theoretical simulations, we correspondingly adopt a dynamic model (Figure 15), which involves the successive formation of two intermediates, **I**₁ and **I**₂, from the non-activated precursor **R**. The first product **P**₁ is formed together with the intermediate **I**₁, whereas the second product **P**₂ results from the reaction of the intermediate **I**₂.

Figure 16a–d display the simulated temporal evolution of the concentrations of the products **P**₁ and **P**₂ when activation occurs in a closed homogeneous system with different values for the rate constants associated to the activation (k_a) and liberation ($k_{1,1}$ and $k_{1,2}$)

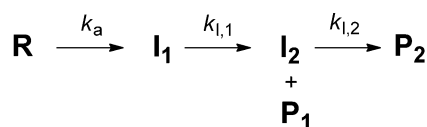


Figure 15. The **R****I**₁**I**₂**P**₁**P**₂ kinetic model.

steps. The liberation of the product **P**₁ exhibits similar features to the **P** liberation discussed in Figure 12: **P**₁ liberation occurs after a delay τ_a when $k_{1,1} < k_a$. **P**₂ liberation subsequently takes place either with a delay (when $\tau_{1,1} = 1/k_{1,1} < \tau_{1,2} = 1/k_{1,2}$) or not (when $\tau_{1,1} = 1/k_{1,1} > \tau_{1,2} = 1/k_{1,2}$).

The preceding considerations have been relevant to design branched self-immolative spacers bearing two leaving groups without any significant delay between the two product liberations.^[73,149,150] In particular, a caged dual branched self-immolative spacer was used to build a caging platform with fluorescence reporting, which was shown to be efficient and versatile for various biological applications.^[73] In this system, it was crucial to design the self-immolative spacer to reduce the delay between the liberations of the substrate and the fluorescent reporter as much as possible (Figure 17).

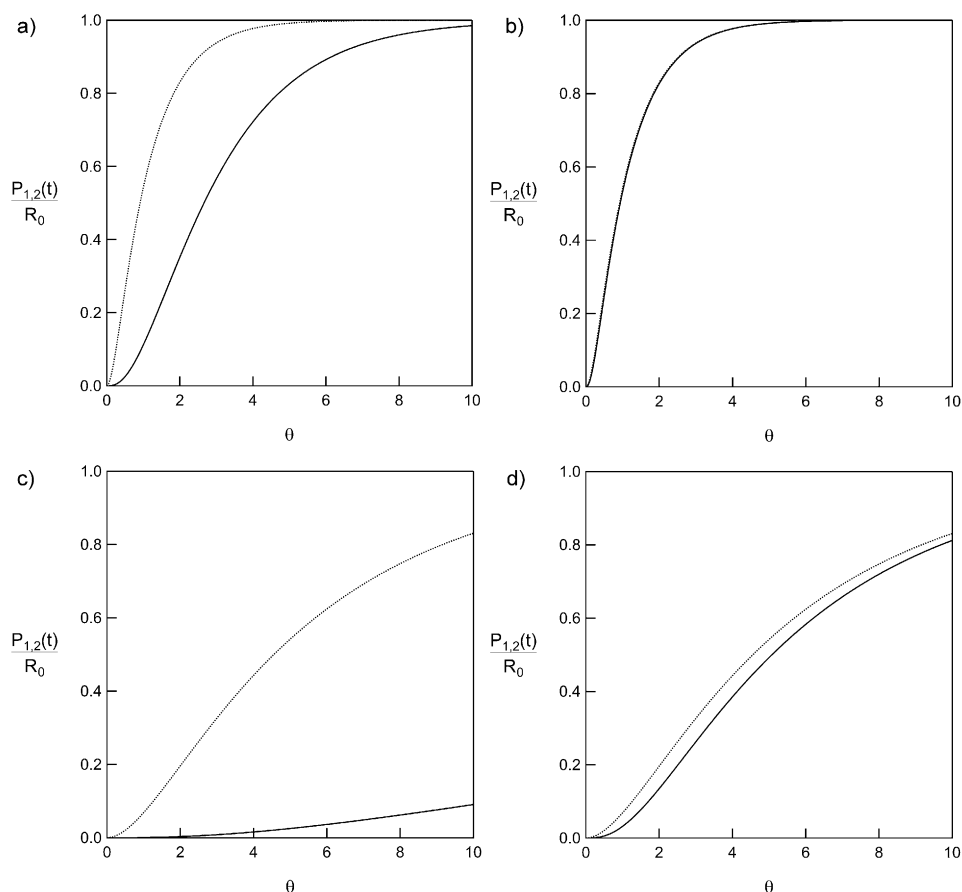


Figure 16. Temporal evolution of the concentrations in the products **P**₁ (dotted line) and **P**₂ (solid line); normalized to the initial concentration R_0 of the non-activated precursor) associated to the dynamic model shown in Figure 15: $(P_1(t)/R_0) = [k_a/(k_{1,1} - k_a)][(\exp(-k_a t) - \exp(-k_{1,1} t))]$; $P_2(t)/R_0 = 1 - \{k_{1,1}k_{1,2}\exp(-k_a t)/[(k_{1,1} - k_a)(k_{1,2} - k_a)] + k_a k_{1,2}\exp(-k_{1,1} t)/[(k_a - k_{1,1})(k_{1,2} - k_{1,1})] + k_a k_{1,1}\exp(-k_{1,2} t)/[(k_a - k_{1,2})(k_{1,1} - k_{1,2})]\}$. The temporal evolution is plotted as a function of $\theta = t/\tau_a$ for different values of $(k_{1,1}/k_a, k_{1,2}/k_a)$: a) (5, 0.1); b) (5, 10); c) (0.2, 0.1); d) (0.2, 10). See References [53, 73] for the derivation of the kinetic equations.

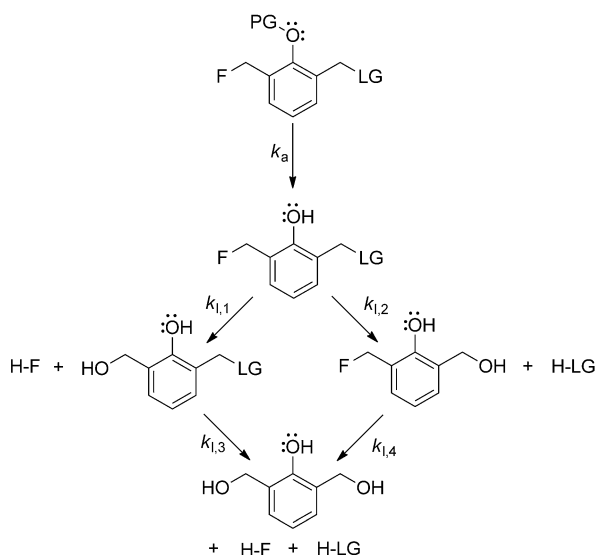


Figure 17. A caging group with a fluorescent reporter based on a self-immolative spacer. The various rate constants $k_{1,i}$ ($i=1-4$) have to be tailored to reduce the delay between the liberations of the substrate and its reporter. PG = Photolabile protecting group; LG = Leaving group belonging to the substrate; F = Fluorescent reporter.

6. Conclusion

This Review has shown that self-immolative spacers already exhibit a wide scope of kinetic properties. In particular, from literature, it is often possible to identify the specific chemistries and molecular architectures required to reach a desired function linked to molecule delivery or material degradation. However, beyond the available repertoire of self-immolative spacers, it is clear that the broader field of kinetically programmed disassembling molecular structures is only beginning to fulfill its potential. In this perspective, it is worth to conclude with two remarks.

First, in the course of the history of chemistry, degradation has attracted the attention of chemists much less than synthesis. In relation to sustainable development, it can be anticipated that programmable self-destruction of molecules or materials will become a main chemical concern. Nature paves the way to clever degradation strategies. However, no doubt the imagination of chemists will further expand the repertoire of disassembling chemistries after molecular activation.

Second, to date, the kinetic demand placed on self-immolative spacers has remained modest. Most applications are presently restricted to introducing a delay for molecular delivery or to achieve spatio-temporal correlation between precursor activation and molecular delivery. These goals have been addressed by relying on simple kinetic schemes involving irreversible unimolecular steps and molecular diffusion. In fact, chemical kinetics definitively provides far richer opportunities. Equipped with non-linear steps, appropriately tailored complex self-immolation mechanisms could yield improved as well as unprecedented controls over molecular delivery or material degradation both in time and in space.

Here again, chemists are expected to find unexplored frontiers to exert their science and imagination.

This work was supported by the French ANR (Kituse, France BioImaging, Morphoscope2).

How to cite: *Angew. Chem. Int. Ed.* **2015**, *54*, 7492–7509
Angew. Chem. **2015**, *127*, 7600–7619

- [1] W. A. Denny, *Future Oncol.* **2010**, *6*, 419–428.
- [2] N. Schellmann, P. M. Deckert, D. Bachran, H. Fuchs, C. Bachran, *Mini-Rev. Med. Chem.* **2010**, *10*, 887–904.
- [3] J. S. Sohn, J. I. Jin, M. Hess, B. W. Jo, *Polym. Chem.* **2010**, *1*, 778–792.
- [4] F. Kratz, I. A. Müller, C. Ryppa, A. Warnecke, *ChemMedChem* **2008**, *3*, 20–53.
- [5] N. J. Harper, *J. Med. Pharm. Chem.* **1959**, *1*, 467–500.
- [6] A. K. Sinhababu, D. R. Thakker, *Adv. Drug Delivery Rev.* **1996**, *19*, 241–273.
- [7] V. J. Stella, K. J. Himmelstein, *J. Med. Chem.* **1980**, *23*, 1275–1282.
- [8] J. Rautio, H. Kumpulainen, T. Heimbach, R. Oliyai, D. Oh, T. Jarvinen, J. Savolainen, *Nat. Rev. Drug Discovery* **2008**, *7*, 255–270.
- [9] P. K. Chakravarty, P. L. Carl, M. J. Weber, J. A. Katzenellenbogen, *J. Med. Chem.* **1983**, *26*, 638–644.
- [10] F. M. de Groot, A. C. de Bart, J. H. Verheijen, H. W. Scheeren, *J. Med. Chem.* **1999**, *42*, 5277–5283.
- [11] P. L. Carl, P. K. Chakravarty, J. A. Katzenellenbogen, *J. Med. Chem.* **1981**, *24*, 479–480.
- [12] C. A. Blencowe, A. T. Russell, F. Greco, W. Hayes, D. W. Thornthwaite, *Polym. Chem.* **2011**, *2*, 773–790.
- [13] A. D. Wong, M. A. DeWit, E. R. Gillies, *Adv. Drug Delivery Rev.* **2012**, *64*, 1031–1045.
- [14] G. I. Peterson, M. B. Larsen, A. J. Boydston, *Macromolecules* **2012**, *45*, 7317–7328.
- [15] D. Shan, M. G. Nicolaou, R. T. Borchardt, B. Wang, *J. Pharm. Sci.* **1997**, *86*, 765–767.
- [16] R. E. Wang, F. Costanza, Y. Niu, H. Wu, Y. Hu, W. Hang, Y. Sun, J. Cai, *J. Controlled Release* **2012**, *159*, 154–163.
- [17] S. Gnaim, D. Shabat, *Acc. Chem. Res.* **2014**, *47*, 2970–2984.
- [18] W. S. Saari, J. E. Schwering, P. A. Lyle, S. J. Smith, E. L. Engelhardt, *J. Med. Chem.* **1990**, *33*, 97–101.
- [19] P. D. Senter, W. E. Pearce, R. S. Greenfield, *J. Org. Chem.* **1990**, *55*, 2975–2978.
- [20] H. J. Schuster, B. Krewer, J. M. von Hof, K. Schmuck, I. Schubert, F. Alves, L. F. Tietze, *Org. Biomol. Chem.* **2010**, *8*, 1833–1842.
- [21] K. A. Ajaj, F. Kratz, *Bioorg. Med. Chem. Lett.* **2009**, *19*, 995–1000.
- [22] Y. L. Leu, C. S. Chen, Y. J. Wu, J. W. Chern, *J. Med. Chem.* **2008**, *51*, 1740–1746.
- [23] C. Antczak, J. S. Jaggi, C. V. LeFave, M. J. Curcio, M. R. McDevitt, D. A. Scheinberg, *Bioconjugate Chem.* **2006**, *17*, 1551–1560.
- [24] A. El Alaoui, N. Saha, F. Schmidt, C. Monneret, J. C. Florent, *Bioorg. Med. Chem.* **2006**, *14*, 5012–5019.
- [25] B. E. Toki, C. G. Cerveny, A. F. Wahl, P. D. Senter, *J. Org. Chem.* **2002**, *67*, 1866–1872.
- [26] S. Chen, X. Zhao, J. Chen, J. Chen, L. Kuznetsova, S. S. Wong, I. Ojima, *Bioconjugate Chem.* **2010**, *21*, 979–987.
- [27] P. J. Burke, P. D. Senter, D. W. Meyer, J. B. Miyamoto, M. Anderson, B. E. Toki, G. Manikumar, M. C. Wani, D. J. Kroll, S. C. Jeffrey, *Bioconjugate Chem.* **2009**, *20*, 1242–1250.
- [28] S. K. Kumar, S. A. Williams, J. T. Isaacs, S. R. Denmeade, S. R. Khan, *Bioorg. Med. Chem.* **2007**, *15*, 4973–4984.

- [29] R. Madec-Lougerstay, J.-C. Florent, C. Monneret, *J. Chem. Soc. Perkin Trans. 1* **1999**, 1369–1376.
- [30] F. Schmidt, J. C. Florent, C. Monneret, R. Straub, J. Czech, M. Gerken, K. Bosslet, *Bioorg. Med. Chem. Lett.* **1997**, 7, 1071–1076.
- [31] A. B. Mauger, P. J. Burke, H. H. Somani, F. Friedlos, R. J. Knox, *J. Med. Chem.* **1994**, 37, 3452–3458.
- [32] A. Satyam, *Bioorg. Med. Chem. Lett.* **2008**, 18, 3196–3199.
- [33] I. F. Antunes, H. J. Haisma, P. H. Elsinga, R. A. Dierckx, E. F. de Vries, *Bioconjugate Chem.* **2010**, 21, 911–920.
- [34] Y. Meyer, J. A. Richard, B. Delest, P. Noack, P. Y. Renard, A. Romieu, *Org. Biomol. Chem.* **2010**, 8, 1777–1780.
- [35] L. Louise-Leriche, E. Paunescu, G. Saint-Andre, R. Baati, A. Romieu, A. Wagner, P. Y. Renard, *Chem. Eur. J.* **2010**, 16, 3510–3523.
- [36] Y. Meyer, J. A. Richard, M. Massonneau, P. Y. Renard, A. Romieu, *Org. Lett.* **2008**, 10, 1517–1520.
- [37] B. Zhu, X. Zhang, H. Jia, Y. Li, H. Liu, W. Tan, *Org. Biomol. Chem.* **2010**, 8, 1650–1654.
- [38] J. A. Richard, Y. Meyer, V. Jolivel, M. Massonneau, R. Dumeunier, D. Vaudry, H. Vaudry, P. Y. Renard, A. Romieu, *Bioconjugate Chem.* **2008**, 19, 1707–1718.
- [39] J. A. Richard, L. Jean, A. Romieu, M. Massonneau, P. Noack-Fraissignes, P. Y. Renard, *Org. Lett.* **2007**, 9, 4853–4855.
- [40] N.-H. Ho, R. Weissleder, C.-H. Tung, *ChemBioChem* **2007**, 8, 560–566.
- [41] X. B. Zhang, M. Waibel, J. Hasserodt, *Chem. Eur. J.* **2010**, 16, 792–795.
- [42] M. Shamis, H. N. Lode, D. Shabat, *J. Am. Chem. Soc.* **2004**, 126, 1726–1731.
- [43] M. Grinda, J. Clarhaut, B. Renoux, I. Tranoy-Opalinski, S. Papot, *MedChemComm* **2012**, 3, 68–70.
- [44] R. Weinstein, E. Segal, R. Satchi-Fainaro, D. Shabat, *Chem. Commun.* **2010**, 46, 553–555.
- [45] R. J. Amir, M. Popkov, R. A. Lerner, C. F. Barbas III, D. Shabat, *Angew. Chem. Int. Ed.* **2005**, 44, 4378–4381; *Angew. Chem.* **2005**, 117, 4452–4455.
- [46] A. Gopin, S. Ebner, B. Attali, D. Shabat, *Bioconjugate Chem.* **2006**, 17, 1432–1440.
- [47] E. Sella, D. Shabat, *J. Am. Chem. Soc.* **2009**, 131, 9934–9936.
- [48] M. Avital-Shmilovici, D. Shabat, *Bioorg. Med. Chem.* **2010**, 18, 3643–3647.
- [49] E. Sella, D. Shabat, *Chem. Commun.* **2008**, 5701–5703.
- [50] S. T. Phillips, A. M. DiLauro, *ACS Macro Lett.* **2014**, 3, 298–304.
- [51] S. T. Phillips, J. S. Robbins, A. M. DiLauro, M. G. Olah, *J. Appl. Polym. Sci.* **2014**, 131, 40992.
- [52] H. Y. Lee, X. Jiang, D. Lee, *Org. Lett.* **2009**, 11, 2065–2068.
- [53] A. Alouane, R. Labruere, T. Le Saux, I. Aujard, S. Dubruille, F. Schmidt, L. Jullien, *Chem. Eur. J.* **2013**, 19, 11717–11724.
- [54] A. Alouane, R. Labruere, K. J. Silvestre, T. Le Saux, F. Schmidt, L. Jullien, *Chem. Asian J.* **2014**, 9, 1334–1340.
- [55] R. Erez, D. Shabat, *Org. Biomol. Chem.* **2008**, 6, 2669–2672.
- [56] F. M. de Groot, C. Albrecht, R. Koekkoek, P. H. Beusker, H. W. Scheeren, *Angew. Chem. Int. Ed.* **2003**, 42, 4490–4494; *Angew. Chem.* **2003**, 115, 4628–4632.
- [57] M. Shamis, D. Shabat, *Chem. Eur. J.* **2007**, 13, 4523–4528.
- [58] F. M. de Groot, W. J. Loos, R. Koekkoek, L. W. van Berkum, G. F. Busscher, A. E. Seelen, C. Albrecht, P. de Bruijn, H. W. Scheeren, *J. Org. Chem.* **2001**, 66, 8815–8830.
- [59] M. A. Dewit, E. R. Gillies, *J. Am. Chem. Soc.* **2009**, 131, 18327–18334.
- [60] M. A. DeWit, E. R. Gillies, *Org. Biomol. Chem.* **2011**, 9, 1846–1854.
- [61] M. A. Dewit, A. Beaton, E. R. Gillies, *J. Polym. Sci. Part A* **2010**, 48, 3977–3985.
- [62] R. B. Greenwald, Y. H. Choe, C. D. Conover, K. Shum, D. Wu, M. Royzen, *J. Med. Chem.* **2000**, 43, 475–487.
- [63] C. de Gracia Lux, C. L. McFearin, S. Joshi-Barr, J. Sankaranarayanan, N. Fomina, A. Almutairi, *ACS Macro Lett.* **2012**, 1, 922–926.
- [64] B. F. Cain, *J. Org. Chem.* **1976**, 41, 2029–2031.
- [65] U. Grether, H. Waldmann, *Angew. Chem. Int. Ed.* **2000**, 39, 1629–1632; *Angew. Chem.* **2000**, 112, 1688–1691.
- [66] U. Grether, H. Waldmann, *Chem. Eur. J.* **2001**, 7, 959–971.
- [67] A. Zheng, D. Shan, B. Wang, *J. Org. Chem.* **1998**, 64, 156–161.
- [68] A. Zheng, D. Shan, X. Shi, B. Wang, *J. Org. Chem.* **1999**, 64, 7459–7466.
- [69] M. N. Levine, R. T. Raines, *Chem. Sci.* **2012**, 3, 2412–2420.
- [70] S. Milstien, L. A. Cohen, *J. Am. Chem. Soc.* **1972**, 94, 9158–9165.
- [71] R. M. Kevitch, C. S. Shanahan, D. V. McGrath, *New J. Chem.* **2012**, 36, 492–505.
- [72] M. Eigen, L. de Mayer, *Relaxation Methods in Techniques of Organic Chemistry, Vol. VIII, 2nd ed.*, Interscience, New York, London, **1963**, pp. 895–1054.
- [73] R. Labruere, A. Alouane, T. Le Saux, I. Aujard, P. Pelupessy, A. Gautier, S. Dubruille, F. Schmidt, L. Jullien, *Angew. Chem. Int. Ed.* **2012**, 51, 9344–9347; *Angew. Chem.* **2012**, 124, 9478–9481.
- [74] M. J. Pilling, P. W. Seakins, *Reaction Kinetics, 2nd ed.*, Oxford Science, Oxford, **1996**.
- [75] J. I. Steinfeld, J. S. Francisco, W. L. Hase, *Chemical Kinetics and Dynamics, 2nd ed.*, Prentice Hall, New York, **1998**.
- [76] S. Arumugam, V. V. Popik, *J. Org. Chem.* **2010**, 75, 7338–7346.
- [77] A. Warnecke, F. Kratz, *J. Org. Chem.* **2008**, 73, 1546–1552.
- [78] M. P. Hay, B. M. Sykes, W. A. Denny, C. J. O'Connor, *J. Chem. Soc. Perkin Trans. 1* **1999**, 2759–2770.
- [79] B. M. Sykes, M. P. Hay, D. Bohinc-Herceg, N. A. Helsby, C. J. O'Connor, W. A. Denny, *J. Chem. Soc. Perkin Trans. 1* **2000**, 1601–1608.
- [80] M. L. Szalai, R. M. Kevitch, D. V. McGrath, *J. Am. Chem. Soc.* **2003**, 125, 15688–15689.
- [81] S. Li, M. L. Szalai, R. M. Kevitch, D. V. McGrath, *J. Am. Chem. Soc.* **2003**, 125, 10516–10517.
- [82] A. Ortiz, C. S. Shanahan, D. T. Sisk, S. C. Perera, P. Rao, D. V. McGrath, *J. Org. Chem.* **2010**, 75, 6154–6162.
- [83] W. Seo, S. T. Phillips, *J. Am. Chem. Soc.* **2010**, 132, 9234–9235.
- [84] N. W. Polaske, M. L. Szalai, C. S. Shanahan, D. V. McGrath, *Org. Lett.* **2010**, 12, 4944–4947.
- [85] K. M. Schmid, L. Jensen, S. T. Phillips, *J. Org. Chem.* **2012**, 77, 4363–4374.
- [86] K. M. Schmid, S. T. Phillips, *J. Phys. Org. Chem.* **2013**, 26, 608–610.
- [87] S. Bhuniya, M. H. Lee, H. M. Jeon, J. H. Han, J. H. Lee, N. Park, S. Maiti, C. Kang, J. S. Kim, *Chem. Commun.* **2013**, 49, 7141–7143.
- [88] I. R. Vlahov, G. D. Vite, P. J. Kleindl, Y. Wang, H. K. Santhapuram, F. You, S. J. Howard, S. H. Kim, F. F. Lee, C. P. Leamon, *Bioorg. Med. Chem. Lett.* **2010**, 20, 4578–4581.
- [89] R. A. Mosey, P. E. Floreancig, *Org. Biomol. Chem.* **2012**, 10, 7980–7985.
- [90] J. L. M. Jourden, K. B. Daniel, S. M. Cohen, *Chem. Commun.* **2011**, 47, 7968–7970.
- [91] J. S. Robbins, K. M. Schmid, S. T. Phillips, *J. Org. Chem.* **2013**, 78, 3159–3169.
- [92] O. Redy, E. Kisin-Finfer, E. Sella, D. Shabat, *Org. Biomol. Chem.* **2012**, 10, 710–715.
- [93] E. Sella, A. Lubelski, J. Klafter, D. Shabat, *J. Am. Chem. Soc.* **2010**, 132, 3945–3952.
- [94] J. L. M. Jourden, S. M. Cohen, *Angew. Chem. Int. Ed.* **2010**, 49, 6795–6797; *Angew. Chem.* **2010**, 122, 6947–6949.
- [95] R. Perry-Feigenbaum, E. Sella, D. Shabat, *Chem. Eur. J.* **2011**, 17, 12123–12128.

- [96] R. J. Amir, E. Danieli, D. Shabat, *Chem. Eur. J.* **2007**, *13*, 812–821.
- [97] R. J. Amir, N. Pessah, M. Shamis, D. Shabat, *Angew. Chem. Int. Ed.* **2003**, *42*, 4494–4499; *Angew. Chem.* **2003**, *115*, 4632–4637.
- [98] A. P. Esser-Kahn, N. R. Sottos, S. R. White, J. S. Moore, *J. Am. Chem. Soc.* **2010**, *132*, 10266–10268.
- [99] R. Weinstein, A. Sagi, N. Karton, D. Shabat, *Chem. Eur. J.* **2008**, *14*, 6857–6861.
- [100] R. Weinstein, P. S. Baran, D. Shabat, *Bioconjugate Chem.* **2009**, *20*, 1783–1791.
- [101] K. Haba, M. Popkov, M. Shamis, R. A. Lerner, C. F. Barbas III, D. Shabat, *Angew. Chem. Int. Ed.* **2005**, *44*, 716–720; *Angew. Chem.* **2005**, *117*, 726–730.
- [102] D. Shabat, H. N. Lode, U. Pertl, R. A. Reisfeld, C. Rader, R. A. Lerner, C. F. Barbas III, *Proc. Natl. Acad. Sci. USA* **2001**, *98*, 7528–7533.
- [103] D. Shabat, C. Rader, B. List, R. A. Lerner, C. F. Barbas III, *Proc. Natl. Acad. Sci. USA* **1999**, *96*, 6925–6930.
- [104] J. Sloniec, U. Resch-Genger, A. Hennig, *J. Phys. Chem. B* **2013**, *117*, 14336–14344.
- [105] A. Sagi, E. Segal, R. Satchi-Fainaro, D. Shabat, *Bioorg. Med. Chem.* **2007**, *15*, 3720–3727.
- [106] E. Danieli, D. Shabat, *Bioorg. Med. Chem.* **2007**, *15*, 7318–7324.
- [107] O. Redy, D. Shabat, *J. Controlled Release* **2012**, *164*, 276–282.
- [108] R. Perry-Feigenbaum, P. S. Baran, D. Shabat, *Org. Biomol. Chem.* **2009**, *7*, 4825–4828.
- [109] A. Sagi, R. Weinstein, N. Karton, D. Shabat, *J. Am. Chem. Soc.* **2008**, *130*, 5434–5435.
- [110] N. Karton-Lifshin, U. Vogel, E. Sella, P. H. Seeberger, D. Shabat, B. Lepenies, *Org. Biomol. Chem.* **2013**, *11*, 2903–2910.
- [111] M. Grinda, T. Legigan, J. Clarhaut, E. Peraudeau, I. Tranoy-Opalinski, B. Renoux, M. Thomas, F. Guilhot, S. Papot, *Org. Biomol. Chem.* **2013**, *11*, 7129–7133.
- [112] T. Legigan, J. Clarhaut, I. Tranoy-Opalinski, A. Monvoisin, B. Renoux, M. Thomas, A. Le Pape, S. Lerondel, S. Papot, *Angew. Chem. Int. Ed.* **2012**, *51*, 11606–11610; *Angew. Chem.* **2012**, *124*, 11774–11778.
- [113] J. Park, Y. Kim, *Bioorg. Med. Chem. Lett.* **2013**, *23*, 2332–2335.
- [114] P. Klán, T. Šolomek, C. G. Bochet, A. Blanc, R. Givens, M. Rubina, V. Popik, A. Kostikov, J. Wirz, *Chem. Rev.* **2013**, *113*, 119–191.
- [115] M. L. Szalai, D. V. McGrath, *Tetrahedron* **2004**, *60*, 7261–7266.
- [116] R. M. Kevitch, D. V. McGrath, *New J. Chem.* **2007**, *31*, 1332–1336.
- [117] N. Fomina, C. L. McFearin, M. Sermsakdi, J. M. Morachis, A. Almutairi, *Macromolecules* **2011**, *44*, 8590–8597.
- [118] N. Fomina, C. McFearin, M. Sermsakdi, O. Edigin, A. Almutairi, *J. Am. Chem. Soc.* **2010**, *132*, 9540–9542.
- [119] N. Fomina, C. L. McFearin, A. Almutairi, *Chem. Commun.* **2012**, *48*, 9138–9140.
- [120] E. E. Weinert, R. Dondi, S. Colloredo-Melz, K. N. Frankenfeld, C. H. Mitchell, M. Freccero, S. E. Rokita, *J. Am. Chem. Soc.* **2006**, *128*, 11940–11947.
- [121] I. A. Müller, F. Kratz, M. Jung, A. Warnecke, *Tetrahedron Lett.* **2010**, *51*, 4371–4374.
- [122] E. W. Damen, T. J. Nevalainen, T. J. van den Bergh, F. M. de Groot, H. W. Scheeren, *Bioorg. Med. Chem.* **2002**, *10*, 71–77.
- [123] A. R. Katritzky, A. F. Pozharskii, *Handbook of Heterocyclic Chemistry*, 2nd ed., Pergamon, **2000**.
- [124] S. L. Johnson, D. L. Morrison, *J. Am. Chem. Soc.* **1972**, *94*, 1323–1334.
- [125] M. G. Olah, J. S. Robbins, M. S. Baker, S. T. Phillips, *Macromolecules* **2013**, *46*, 5924–5928.
- [126] M. B. Smith, J. March, *March's advanced organic chemistry. Reactions, mechanisms, and structure*, 6th ed., Wiley, New York, **2007**.
- [127] Y. Kuang, K. Balakrishnan, V. Gandhi, X. Peng, *J. Am. Chem. Soc.* **2011**, *133*, 19278–19281.
- [128] W. Chen, Y. Han, X. Peng, *Chem. Eur. J.* **2014**, *20*, 7410–7418.
- [129] S. Cao, R. Christiansen, X. Peng, *Chem. Eur. J.* **2013**, *19*, 9050–9058.
- [130] I. Tranoy-Opalinski, A. Fernandes, M. Thomas, J. P. Gesson, S. Papot, *Anti-Cancer Agents Med. Chem.* **2008**, *8*, 618–637.
- [131] R. B. Greenwald, C. D. Conover, Y. H. Choe, *Crit. Rev. Ther. Drug Carrier Syst.* **2000**, *17*, 101–161.
- [132] B. Liu, L. Hu, *Bioorg. Med. Chem.* **2003**, *11*, 3889–3899.
- [133] C. Santos, M. L. Mateus, A. P. dos Santos, R. Moreira, E. de Oliveira, P. Gomes, *Bioorg. Med. Chem. Lett.* **2005**, *15*, 1595–1598.
- [134] L. Hu, B. Liu, D. R. Hacking, *Bioorg. Med. Chem. Lett.* **2000**, *10*, 797–800.
- [135] T. C. Bruice, U. K. Pandit, *J. Am. Chem. Soc.* **1960**, *82*, 5858–5865.
- [136] G. J. Atwell, B. M. Sykes, C. J. O'Connor, W. A. Denny, *J. Med. Chem.* **1994**, *37*, 371–380.
- [137] E. K. Y. Chen, R. A. McBride, E. R. Gillies, *Macromolecules* **2012**, *45*, 7364–7374.
- [138] J. Hanusek, M. Sedláč, P. Jansa, V. Štěrba, *J. Phys. Org. Chem.* **2006**, *19*, 61–67.
- [139] C. Percivalle, A. La Rosa, D. Verga, F. Doria, M. Mella, M. Palumbo, M. Di Antonio, M. Freccero, *J. Org. Chem.* **2011**, *76*, 3096–3106.
- [140] M. Nadai, F. Doria, M. Di Antonio, G. Sattin, L. Germani, C. Percivalle, M. Palumbo, S. N. Richter, M. Freccero, *Biochimie* **2011**, *93*, 1328–1340.
- [141] H. Wang, M. S. Wahi, S. E. Rokita, *Angew. Chem. Int. Ed.* **2008**, *47*, 1291–1293; *Angew. Chem.* **2008**, *120*, 1311–1313.
- [142] F. Fakhari, S. E. Rokita, *Nat. Commun.* **2014**, *5*.
- [143] K. D. Bagshaw, *Expert Rev. Anti-Cancer Ther.* **2006**, *6*, 1421–1431.
- [144] O. Greco, G. U. Dachs, *J. Cell. Physiol.* **2001**, *187*, 22–36.
- [145] N. I. Kiskin, D. Ogden, *Eur. Biophys. J.* **2002**, *30*, 571–587.
- [146] M. P. Hay, G. J. Atwell, W. R. Wilson, S. M. Pullen, W. A. Denny, *J. Med. Chem.* **2003**, *46*, 2456–2466.
- [147] M. P. Hay, W. R. Wilson, W. A. Denny, *Bioorg. Med. Chem.* **2005**, *13*, 4043–4055.
- [148] S. U. Hettiarachchi, B. Prasai, R. L. McCarley, *J. Am. Chem. Soc.* **2014**, *136*, 7575–7578.
- [149] S. Cao, Y. Wang, X. Peng, *Chem. Eur. J.* **2012**, *18*, 3850–3854.
- [150] S. Cao, Y. Wang, X. Peng, *J. Org. Chem.* **2014**, *79*, 501–508.

Received: January 5, 2015

Published online: June 5, 2015